Supplementary Information (SI) for Green Chemistry.
This journal is © The Royal Society of Chemistry 2025

Supporting Information:

Overcoming the Conversion Reaction Limitation with Dual-phase Sulfide-based Cathode for All-Solid-State Lithium-Sulfur Batteries

Ruojian Ma,[†a] Yingzuo He,[†a] Minghao Ruan,[†a] Ruyi Fang,*[a] Xinxu Wang,[a] Jun Zhang,[a] Yongping Gan,[a] Xinping He,[a] Hui Huang,[a] Xinhui Xia,[a] Wenkui Zhang,[a] Xinyong Tao,[a] Min Fan[a] and Yang Xia*[a]

[a] *College of Materials Science and Engineering, Zhejiang University of Technology, Hangzhou 310014, China.*

† *These authors contributed equally to this work.*

* *Corresponding Authors: friesfang@zjut.edu.cn (R.Y. Fang); nanoshine@zjut.edu.cn (Y. Xia)*

The electron conductivity was calculated by the equation:

$$\sigma_{e^-} = \frac{d}{S \times R_i}$$

where $\boldsymbol{R_i}$ is the total resistance of the electrode when the current is stable under the external voltage, $\boldsymbol{d}$ is the sample thickness, and $\boldsymbol{S}$ is the area of the electrode.

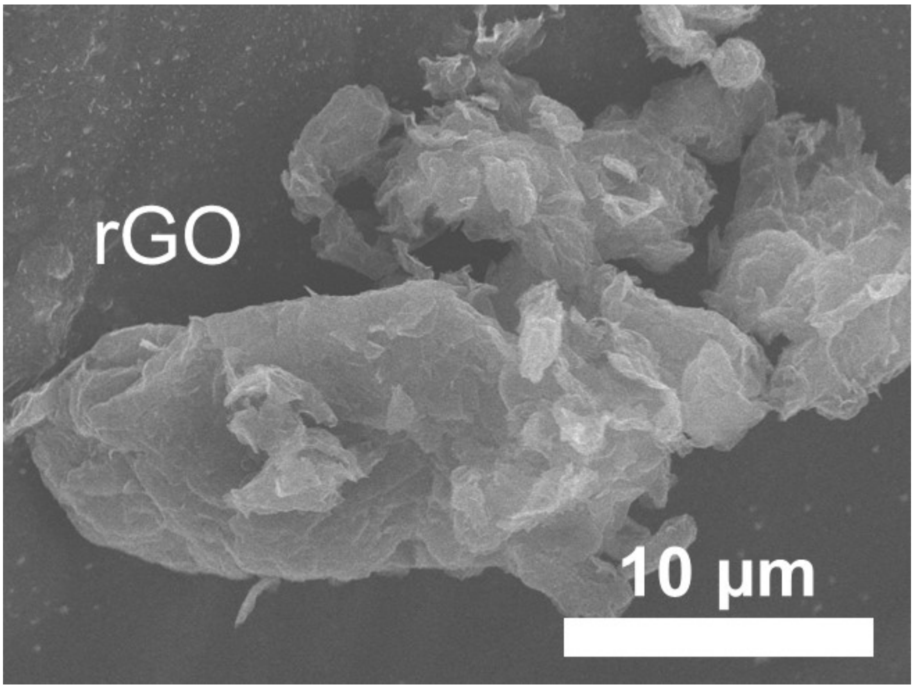

Fig. S1. SEM image of rGO.

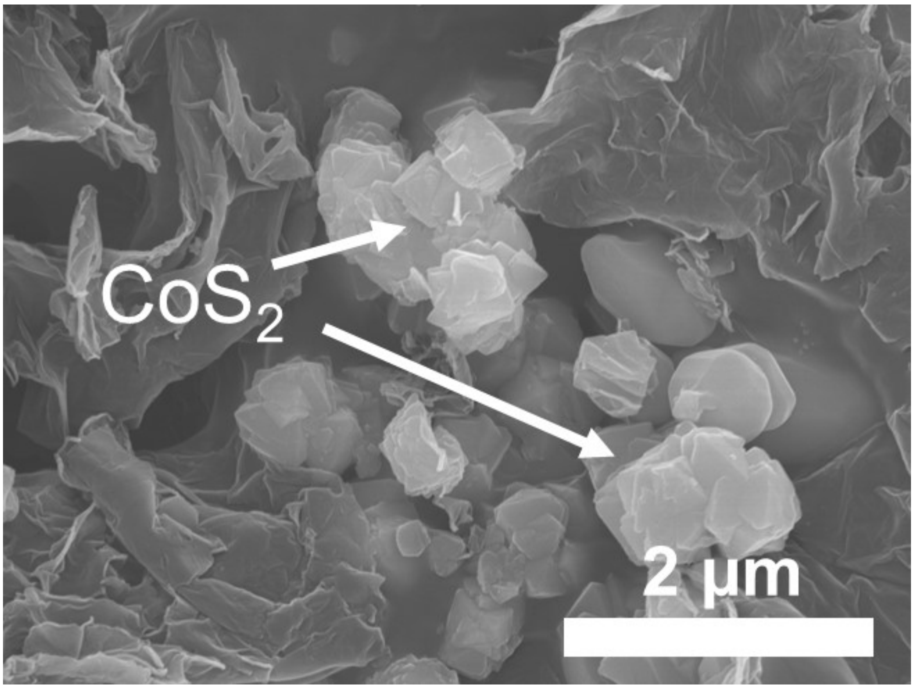

Fig. S2. SEM image of CoS_2@rGO.

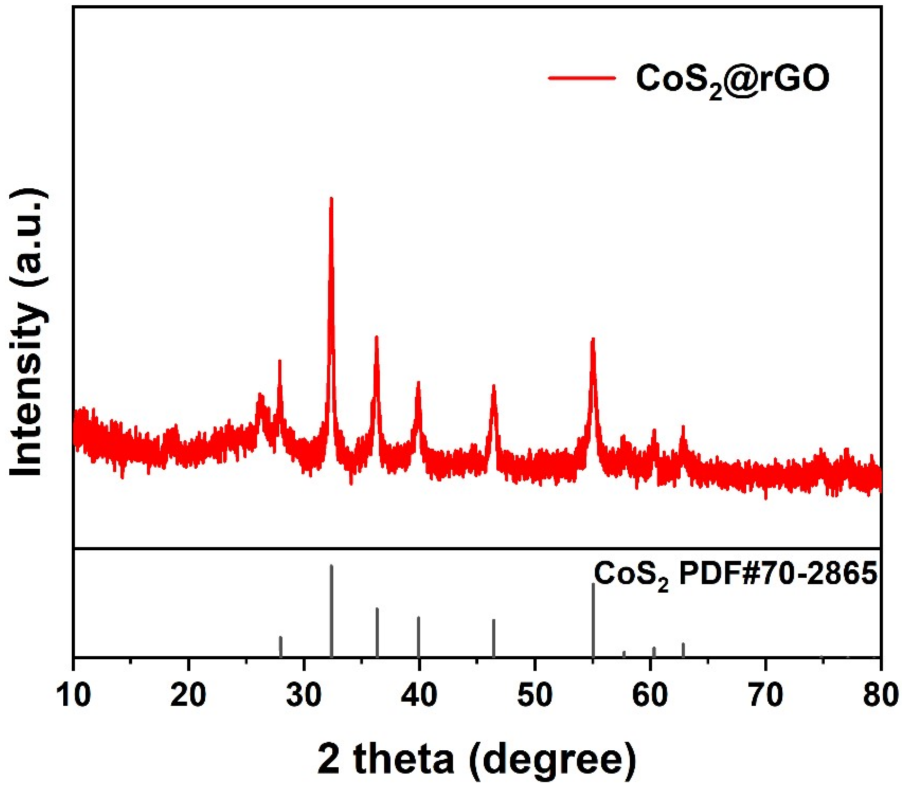

Fig. S3. XRD pattern of CoS_2@rGO.

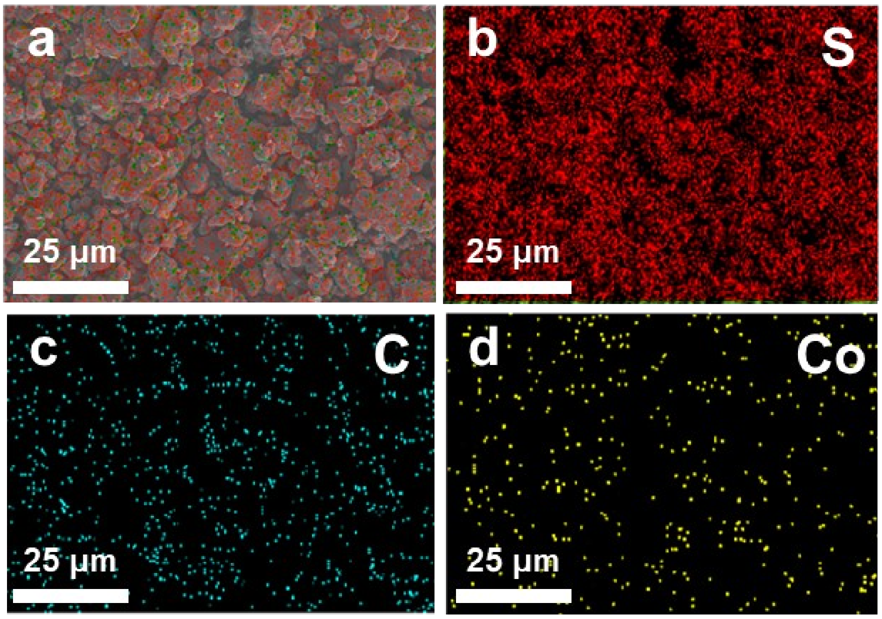

Fig. S4. SEM image of S/CoS_2@rGO**.**

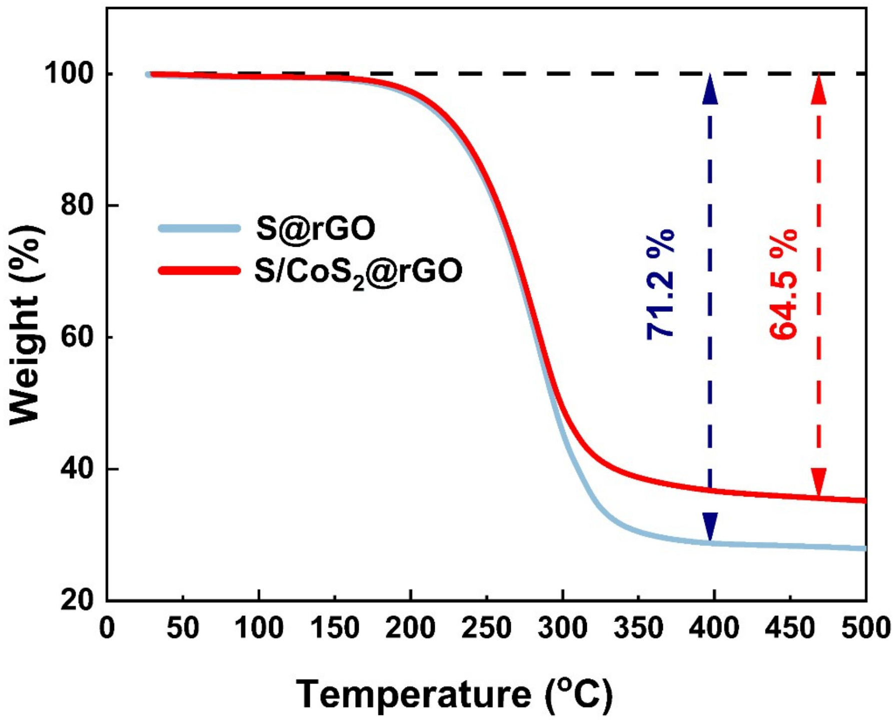

Fig. S5. The TG curves of the S@rGO, and S/CoS_2@rGO cathode material.

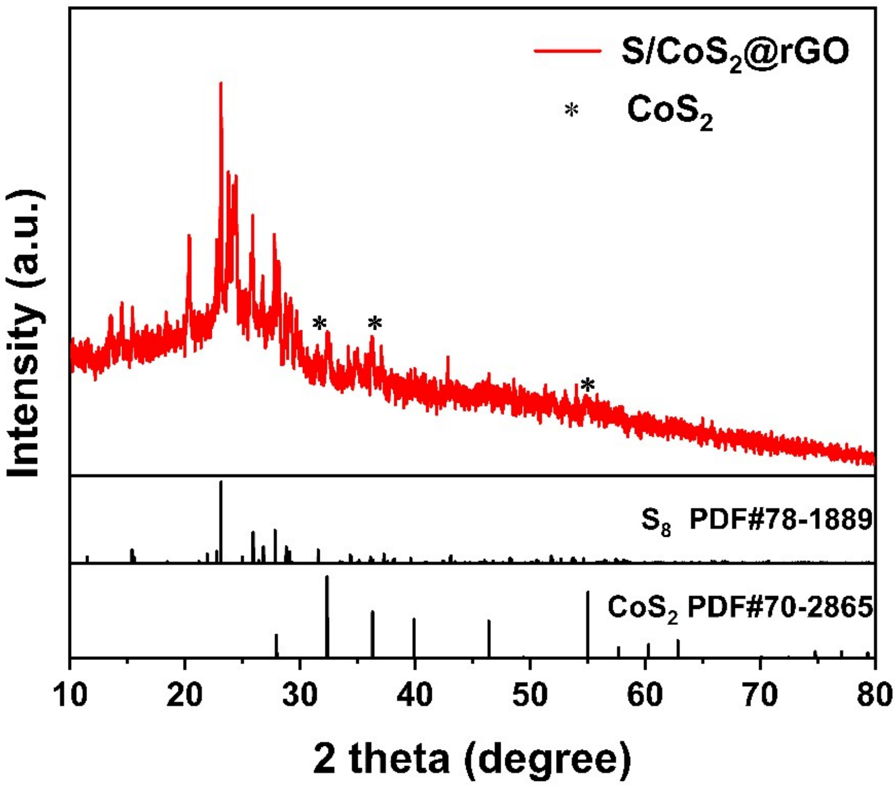

Fig. S6. XRD pattern of $S/CoS_2@rGO$.

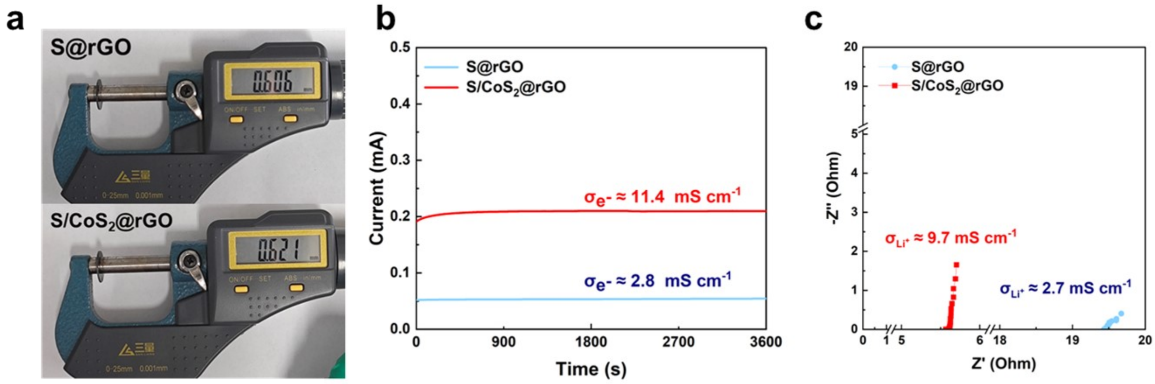

Fig. S7. (a) Digital photographs on the micrometer caliper results. (b) DC polarization curves and (c) the Nyquist plots of the S@rGO and S/CoS_2@rGO at room temperature.

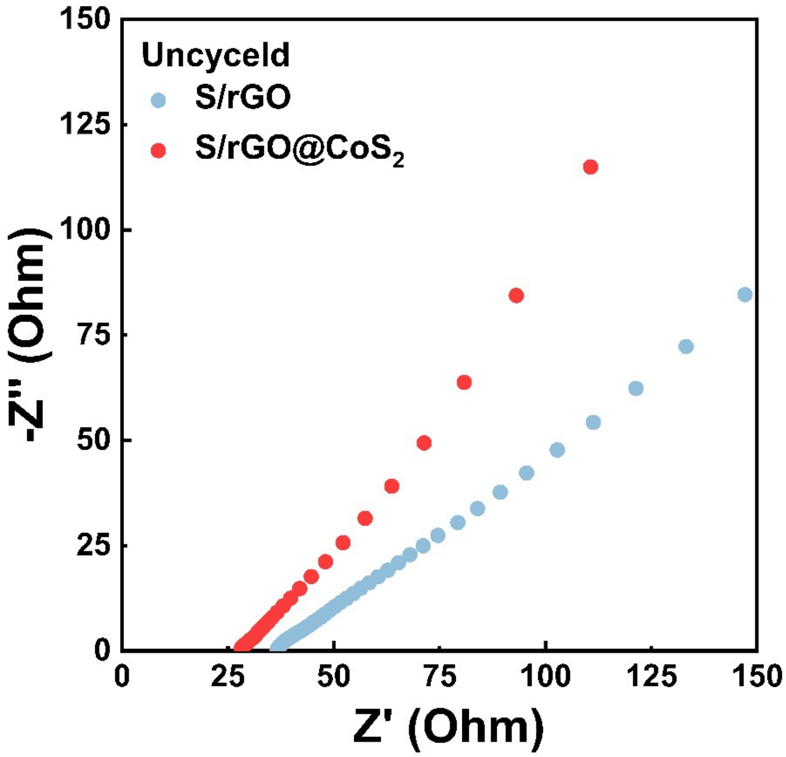

Fig. S8. Comparison between S@rGO and S/CoS_2@rGO on the Nyquist plot before cycling.

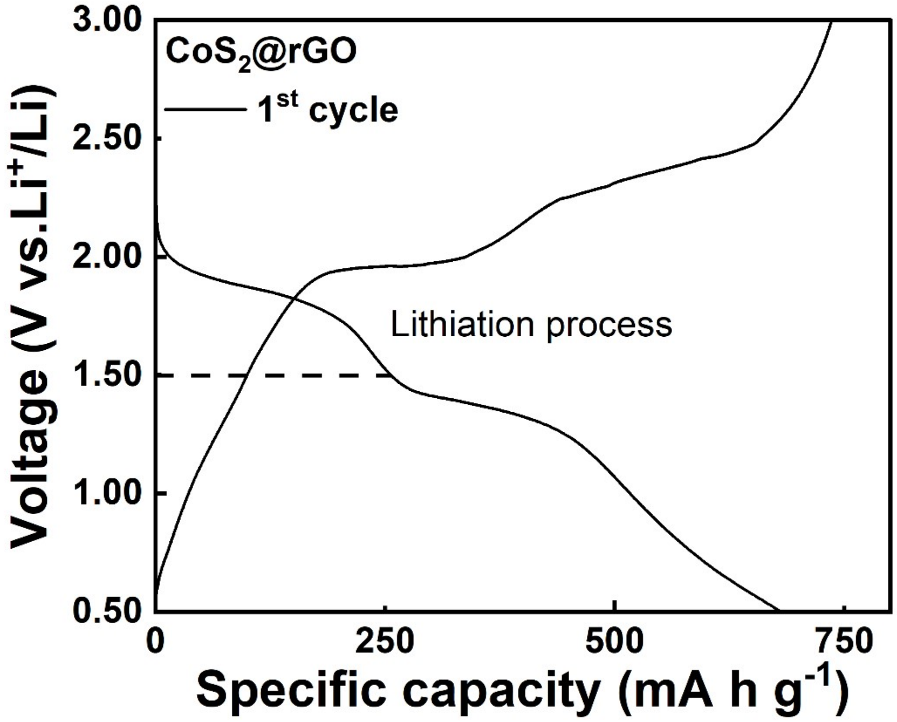

Fig. S9. Charge-discharge curve of CoS_2@rGO in the initial cycle.

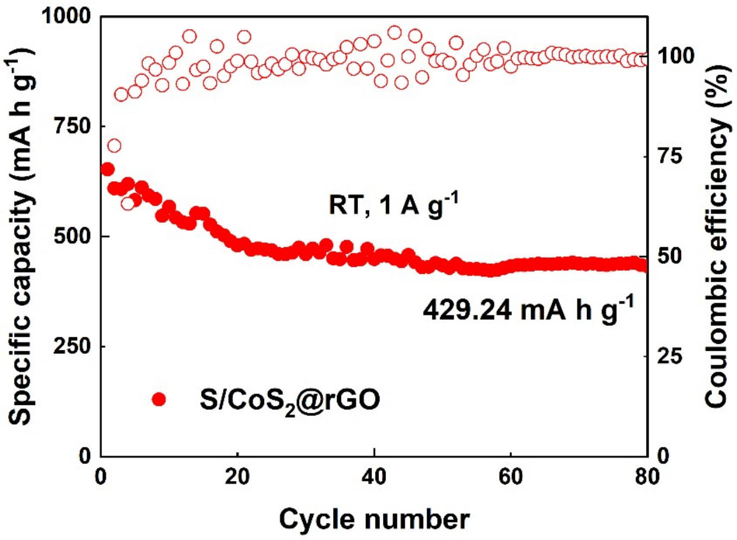

Fig. S10. The cycling performance of the ASSLSBs with S/CoS_2@rGO cathode at 1 A g^{-1}.

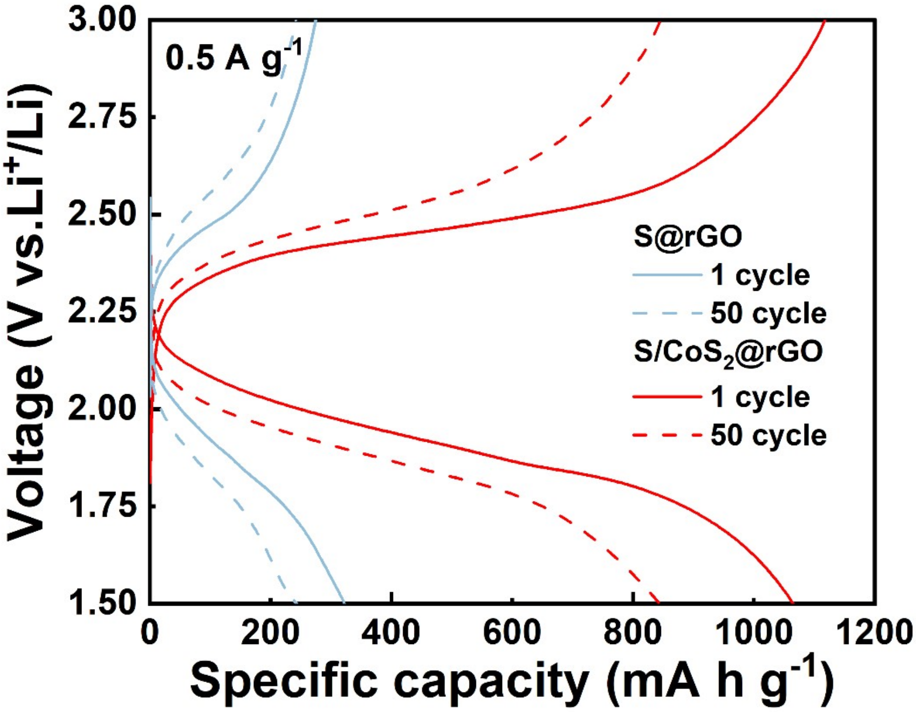

Fig. S11. Comparison between S@rGO and S/CoS_2@rGO on the 1st and 50th charge-discharge curves at 0.5 A g^{-1}.

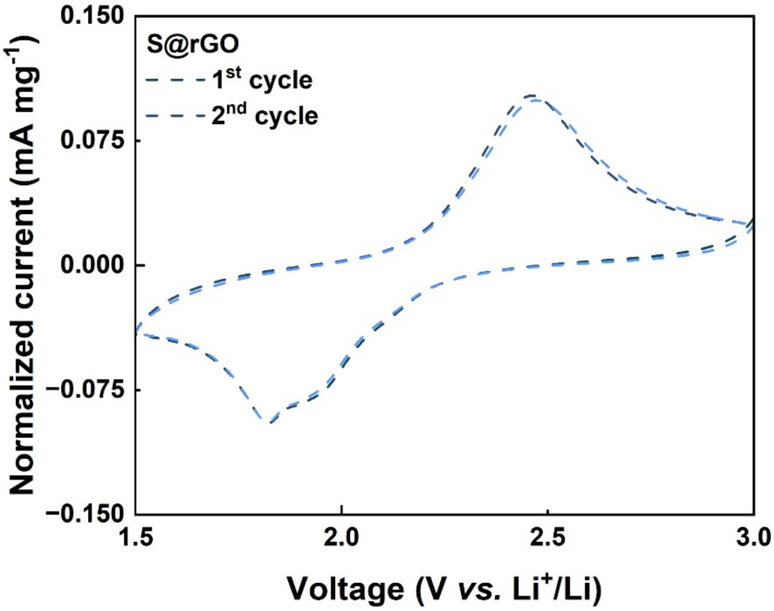

Fig. S12. The CV curves of the ASSLSBs with S@rGO cathode materials.

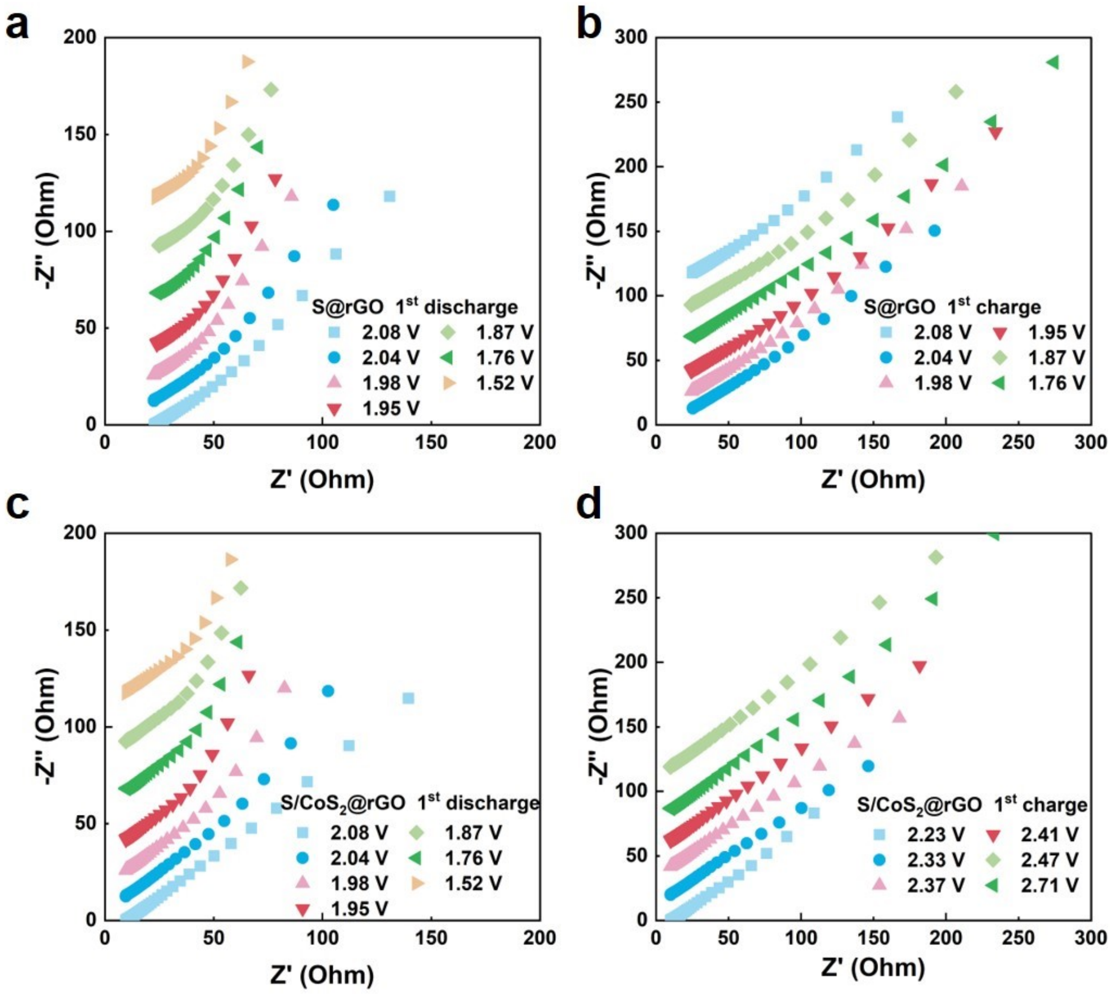

Fig. S13. *In-situ* EIS plots of S@rGO during (a) the initial discharge, (b) the initial charge, and S/CoS_2@rGO during (c) the initial discharge, (d) the initial charge.

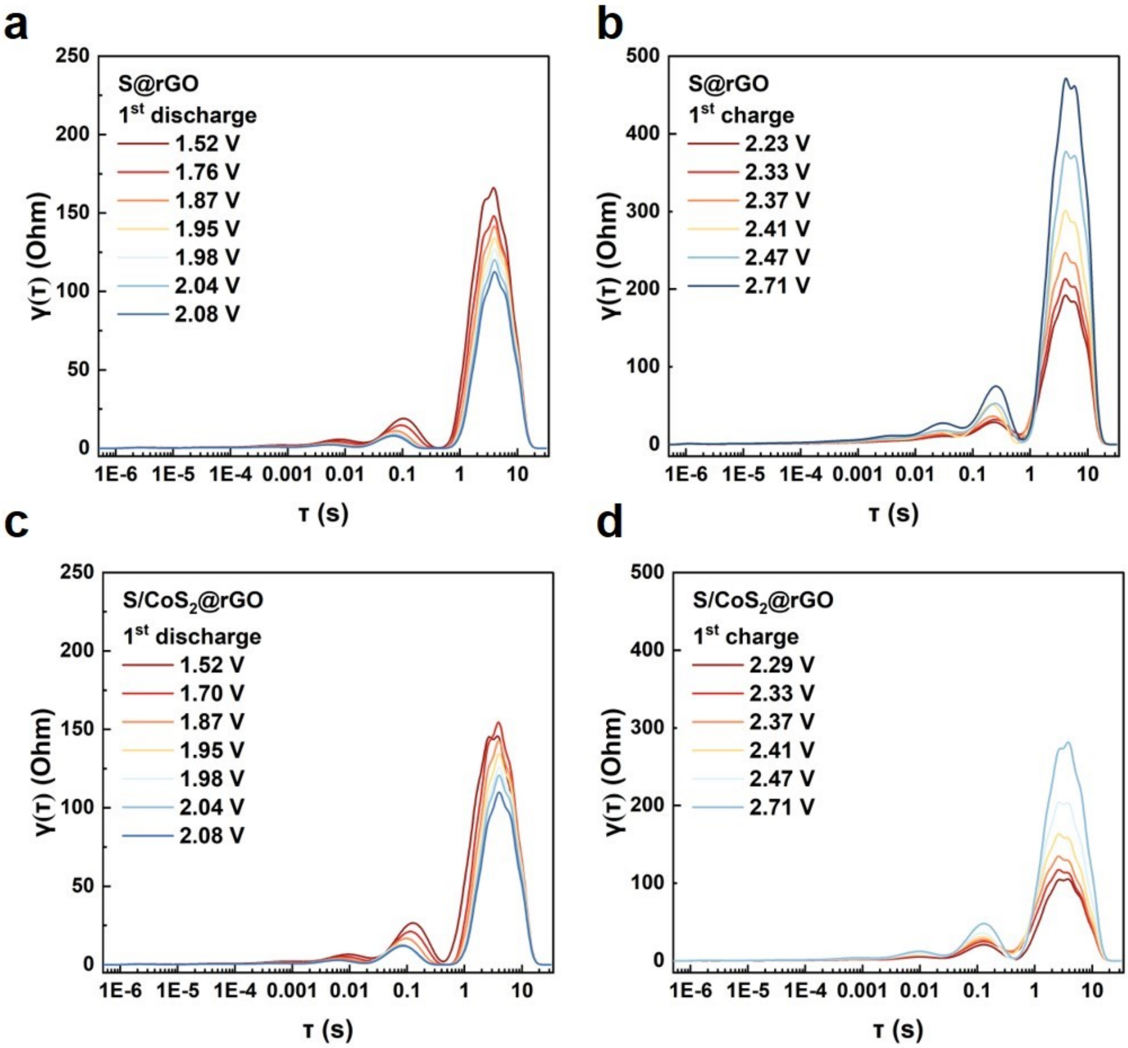

Fig. S14. DRT curves based on the *in-situ* EIS plots of S@rGO during (a) the initial discharge, (b) the initial charge, and S/CoS_2@rGO during (c) the initial discharge, (d) the initial charge.

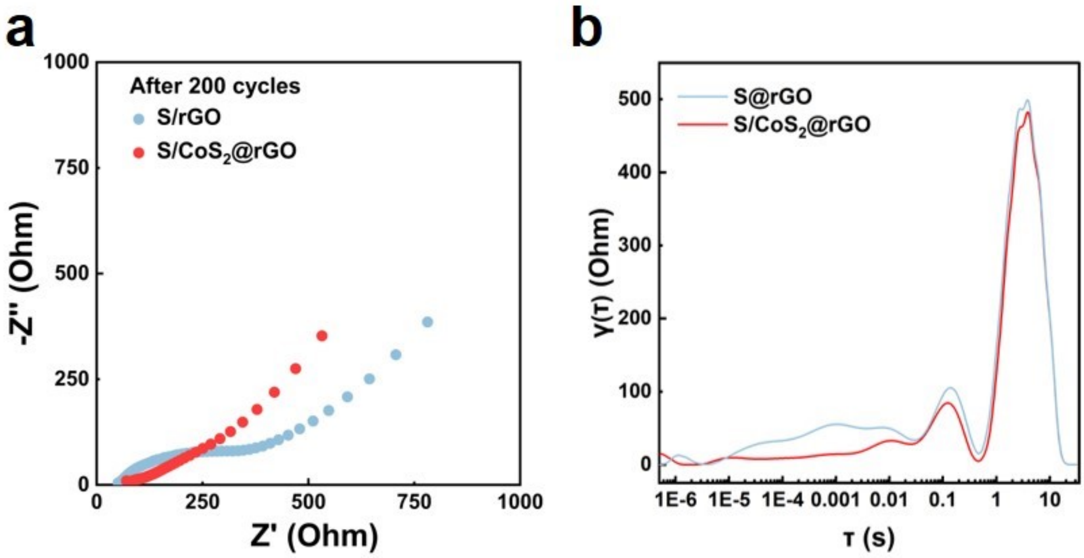

Fig. S15. (a) The Nyquist of the S@rGO and S/CoS_2@rGO after 200 cycles, (b) corresponding DRT curves.

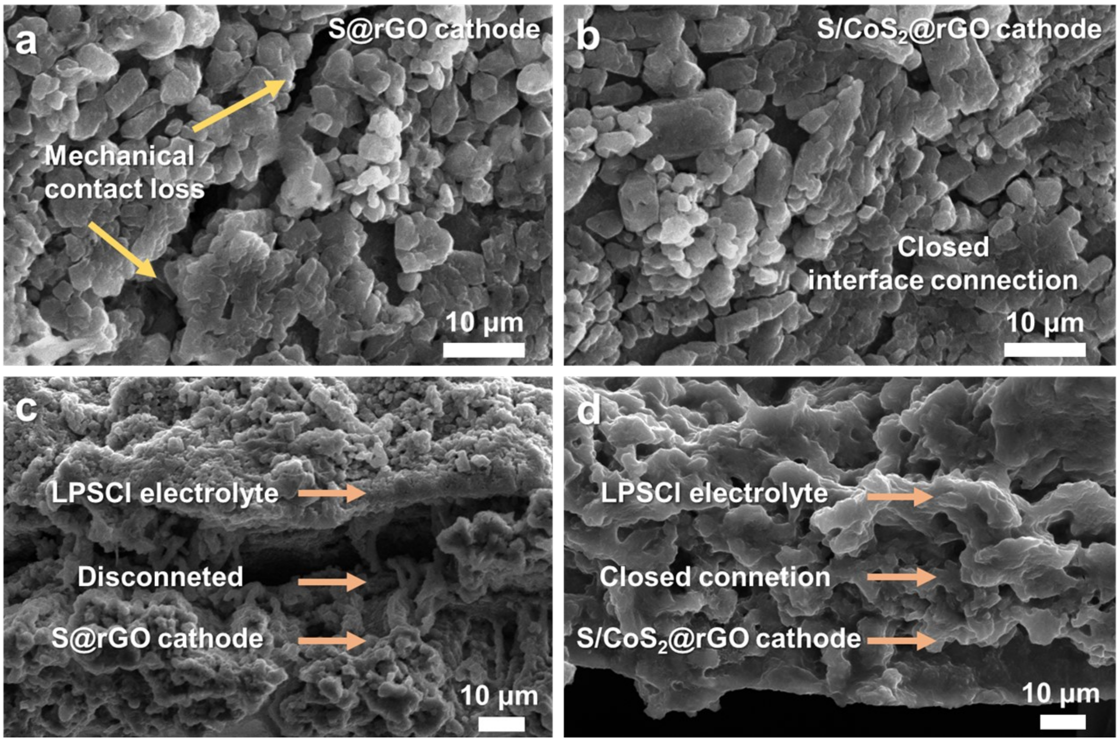

Fig. S16. The post-mortem morphology of (a, c) the S@rGO and (b, d) S/CoS_2@rGO cathode.

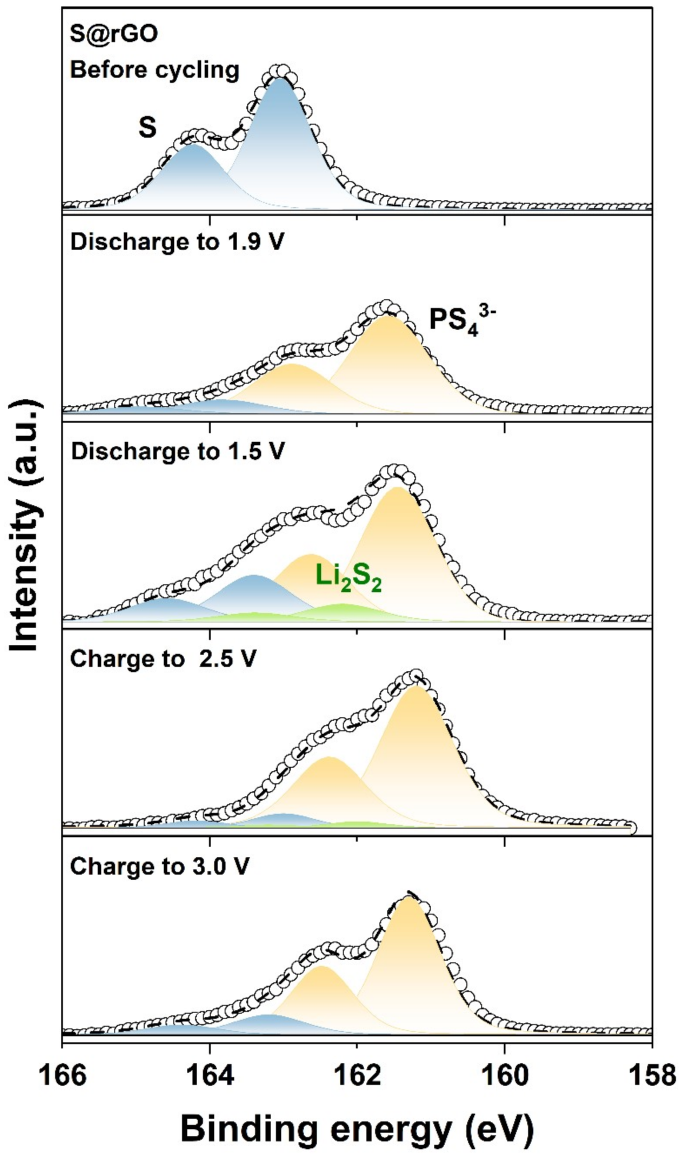

Fig. S17. Ex-situ S 2p spectra of S@rGO cathode during the initial cycle.

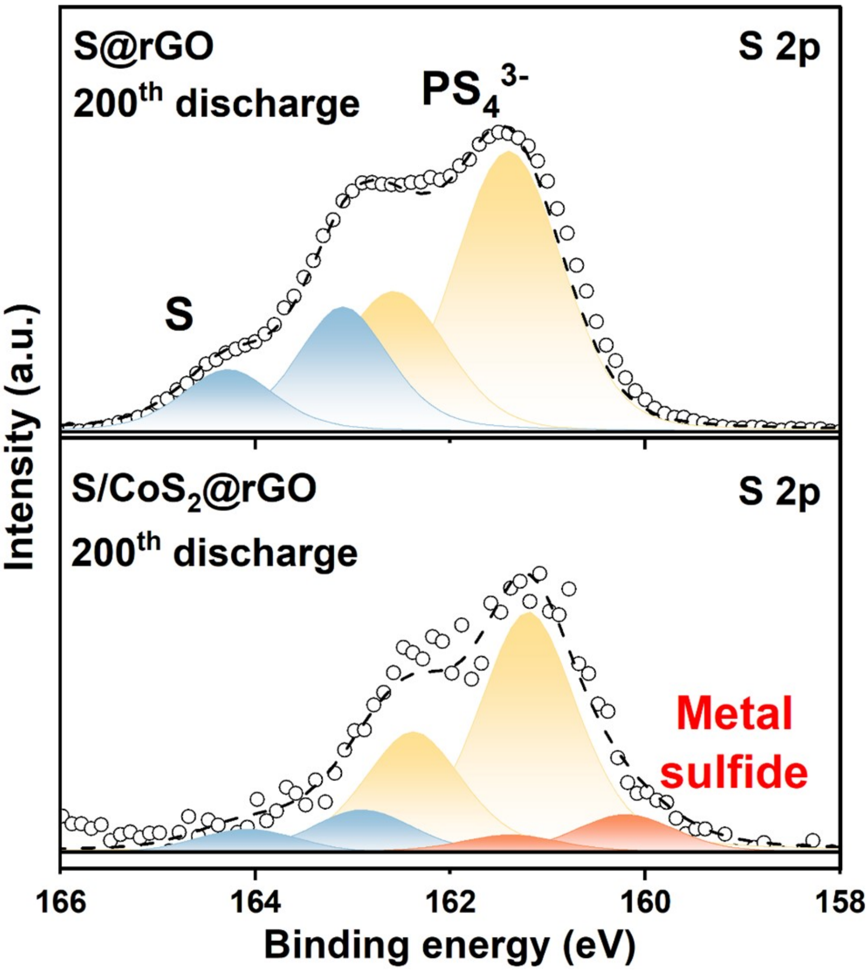

Fig. S18. The S 2p of the S@rGO and S/CoS_2@rGO after the 200th discharge.

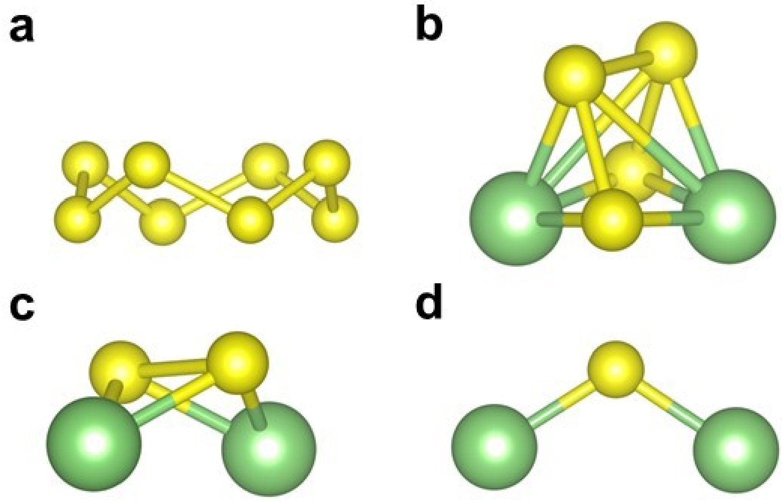

Fig. S19. Configurations of the (a) S, (b) Li_2S_4, (c) Li_2S_2, (d) Li_2S.

Table S1. Element content of S/CoS_2@rGO based on EDX detection.

Element	**Wt%**
C	**29.03**
S	**67.35**
Co	**3.62**
Total：	**100.00**

Table S2 Comparisons to the current state of the art in the electrochemical characteristics and green nature of sulfur cathode

Composite Cathode	Operation condition	Sulfur loading （mg cm⁻²）	Cathode utilization	Capacity ($mA\ h\ g^{-1}$) @ current density	Cycles@ capacity retention	Rate property ($mA\ h\ g^{-1}$) @ current density	Key Green indicator	Ref.
CNT-COPS@S	30 °C 1.6~2.9 V	1.79 ± 0.39	67%	1128@0.1C	100@47%	—	Toxic liquid Low cycling stability	1
S/C/LPSC	60 °C 1.5~2.8V	1	55%	932@0.05C	50@62%	665@0.3C	Limited efficiency Low rate capability	2
SVD-5S@CNT	60 °C 0.8~2.4 V	—	76%	1275@0.1C	100@78%	870@1C	Limited efficiency Low cycling stability	3
10%rGO-VS_4 @$Li_7P_3S_{11}$	25 °C 1.5~3.0 V	2.5–3.0	73%	1229@0.06C	100@93%	473@0.6C	Limited efficiency Low rate capability	4
S/Li_3YCl_5I/CNT	45 °C 1.6~3.1V	1.125	65%	1084@0.01C	200@70%	477@0.5C	Limited efficiency Low rate capability	5
S-In/LPSC/KB	30 °C 0.8~2.4V	3.5	74%	1233@0.05C	1500@50%	885@0.5C	Limited efficiency Low rate capability	6
CNTs@S/AB/ LGPS	60 °C 1.5~2.8V	0.4-0.5	71%	1193@0.1C	20@82%	960@0.5C	Limited efficiency Low cycling stability	7
S/CoS_2@rGO	30 °C 1.5~3.0 V	2.15	98%	1547@0.06C	200@60%	1065@0.3C	Ultra-high efficiency High cycling stability	This work

Reference

1. R. I. Anayah, I. J. Dillingham and V. S. Thoi, *ACS Applied Energy Materials*, 2025, DOI: 10.1021/acsaem.5c00725.
2. J.-K. Hu, H. Yuan, S.-J. Yang, Y. Lu, S. Sun, J. Liu, Y.-L. Liao, S. Li, C.-Z. Zhao and J.-Q. Huang, *Journal of Energy Chemistry*, 2022, **71**, 612-618.
3. W. Si, J. Gao, Y. Gao, F. Zhao, Y. Zhang, X. Sun and J. Wu, *Journal of Energy Storage*, 2024, **97**, 112829.
4. Q. Zhang, H. Wan, G. Liu, Z. Ding, J. P. Mwizerwa and X. Yao, *Nano Energy*, 2019, **57**, 771-782.
5. X. Fang, Y. Fu, S. Sun, R. Zhang, P. Guo, K. Sun, D. Liu, K. Wang and D. He, *Nano Letters*, 2025, **25**, 3843-3850.
6. P. Chen, H. Qu, D. Zheng, X. Zhang and D. Qu, *Advanced Functional Materials*, 2025, DOI: 10.1002/adfm.202423633.
7. Q. Zhang, N. Huang, Z. Huang, L. Cai, J. Wu and X. Yao, *Journal of Energy Chemistry*, 2020, **40**, 151-155.